

A SPEED-SENSORLESS INDIRECT FIELD-ORIENTED CONTROL FOR INDUCTION MOTORS: THEORETICAL RESULT AND EXPERIMENTAL EVALUATION

Introduction. Vector controlled Induction Motor (IM) drives are wide spread electromechanical conversion systems for high dynamic performance applications, where motion control or high precision speed control is needed. Usually, a digital shaft speed-position sensor is required in these applications. For low dynamic applications such as pumps and fans the typical solution is the so called "adjustable-speed" drive. This is a simple low-cost voltage-source inverter fed IM drive with scalar voltage frequency control. Voltage frequency controlled drives typically are speed-sensorless, i.e. without the speed-position sensor, according to common nomenclature in electric drive field.

An intermediate class of AC drive applications such as elevators, auxiliary machines of rolling mills and other technological installations requires enhanced dynamic performances and wider speed range as compared with "adjustable speed" drives, but approximately at the same cost. All leading electrical drive producers have already presented in the market sensorless products even if a theoretical framework for IM sensorless control is not well established yet.

There is a large number of investigations related to this problem. Extensive overviews of AC sensorless control strategies are given in [1] – [4]. According to these references the main contributions are concentrated in three main directions: IM spatial saliency methods with fundamental excitation and high frequency signal injection [5], extended Kalman filter technique [6] and adaptive system approaches. Interest in medium and potentially high performance applications of IM pointed main research efforts in the third direction.

In [7] the authors proposed an output feedback controller which represents a true sensorless solution, since it has the following features: full-order IM model is considered; no flux measurement or estimation, based on open-loop integration, is required; it is based only on stator current measurements, without any differentiation; load torque is assumed constant, but unknown; by replacing the speed estimation with the speed measurement, global exponential stability is achieved (see [8]); control objectives of each control subsystems are clearly understandable and a regular tuning procedure for the controller gains can be adopted.

In this paper the results of intensive experimental and simulation tests are presented in order to demonstrate that the achievable performances are close to those which are typically obtained from standard vector control with speed measurement.

Speed-flux sensorless control algorithm. The general structure and the basic design approach adopted for the proposed speed-flux sensorless controller are the following. The controller is composed by a feed-forward and a feedback part. The feed-forward part is derived from model inversion assuming smooth references. The feedback one is designed exploiting classic cascade structure for inner current and outer speed-flux control loops. Lyapunov design is applied following the conceptual line reported in [8] and introducing a novel speed estimator. The flux controller is based on the improved indirect field-oriented control approach, hence no flux estimation is required. With suitable gain selection, the torque-current tracking and the speed estimation dynamics are imposed much faster than the speed-flux control loops, thus achieving two-time scale property. This feature is crucial for the stability of the overall tracking and estimation error dynamics.

The proposed speed-flux controller and speed estimator are defined as follows:

flux controller

$$\begin{aligned} i_d^* &= \frac{1}{\alpha L_m} (\alpha \psi^* + \dot{\psi}^*); \\ \dot{e}_0 = \omega_0 &= \hat{\omega} + \alpha L_m \frac{i_q}{\psi^*} + \frac{v_q}{\psi^*}, \end{aligned} \quad (1)$$

$$v_q = \frac{1}{\beta} \left[\hat{\omega}(1 + \gamma_1) + \alpha L_m \frac{i_q}{\psi^*} \right] \tilde{i}_d, \quad \gamma_1 = \frac{\left(\frac{R_s}{\sigma} + k_{idl} \right)}{\alpha}, \quad (2)$$

speed controller

$$\begin{aligned} i_q^* &= \frac{1}{\mu \psi^*} \left(\dot{\omega}^* + \hat{T}_L - k_\omega e_\omega \right); \\ \hat{T}_L &= -k_{\omega i} e_\omega, \end{aligned} \quad (3)$$

current controller

$$\begin{aligned} u_d &= \sigma \left(\gamma i_d^* - \omega_0 i_q - \alpha \beta \psi^* + i_d^* - k_{id1} \tilde{i}_d \right); \\ u_q &= \sigma \left(\gamma i_q^* + \omega_0 i_d + \beta \dot{\omega} \psi^* + i_q^* - k_{iq1} \tilde{i}_q \right), \end{aligned} \quad (4)$$

speed estimator

$$\hat{\omega} = \omega^* - k_{i\omega} \tilde{i}_q, \quad (5)$$

where i_d, i_q, u_d, u_q denote components of the stator current and stator voltage vectors. Subscripts d and q stand for vector components in the (d-q) reference frame, and ε_0 is the angular position of the (d-q) reference frame with respect to a fixed stator reference frame (a-b), where the physical variables are defined. Superscript (*) stand for reference trajectories, ω is the rotor speed, $\hat{\omega}$ is the speed estimation, \hat{T}_L is the estimation of load constant T_L/J , T_L is the load torque, $e_\omega = \hat{\omega} - \omega^*$ is the estimated speed tracking error, $\tilde{i}_d = i_d - i_d^*$, $\tilde{i}_q = i_q - i_q^*$ the current tracking errors with respect to references generated by flux and speed controllers, $\psi^* > 0$ is the reference for motor flux vector modulus. Positive constants related to the electrical and mechanical parameters of the IM are defined in a standard way [9]. One pole pair is assumed without loss of generality. No mechanical friction is supposed.

Control tuning parameters in (1)–(5) are the proportional and integral gains of the speed controller $(k_\omega, k_{\omega i})^T > 0$, the proportional gains of the current controllers $(k_{id1}, k_{iq1})^T > 0$, the tuning gain γ_1 and the speed estimator gain $k_{i\omega} > 0$. The correction term v_q in the flux controller (2) is defined using Lyapunov design [7].

Experimental results. The proposed sensorless control algorithm has been experimentally tested using a 1.1 kW standard induction motor whose rated data are the following: power 1.1 kW, speed 1500 rev/min, torque 7.0 Nm, frequency 50 Hz, number of poles 4, excitation current 1.4 A, rated current 2.8 A, $R_s = 10.4$ Ohm, $R_r = 4.5$ Ohm, $L_m = 0.434$ H, $L_s = 0.47$ H, $L_r = 0.47$ H, $J = 0.0034$ Kgm².

Controller tuning. During all the tests the controller parameters are set at constant values: $k_{id1} = 300$, $\gamma_1 = 47$, $k_\omega = 140$, $k_{\omega i} = 9800$, $k_{iq1} = 160$.

Operating sequences. The flux and speed reference trajectories adopted in the experiments are presented in Fig. 1 using solid lines; dashed line in the same figure represents the load torque profile. The operating sequence of the performed tests is the following:

1. The machine is excited during the initial time interval 0-0.096s using a flux reference trajectory starting at $\psi^*(0) = 0.02$ Wb and reaching the motor rated value of 0.86Wb with the first and second derivatives equal to 10Wb/s and 1000Wb/s² correspondingly.

2. The unloaded motor is required to track the speed reference trajectory characterized by the following phases: starting from $t = 0.4$ s with zero initial value, speed reference trajectory reaches 100 rad/s at $t = 0.45$ s; from this time up to $t = 1.3$ s constant speed is imposed; from $t = 1.3$ s the motor is required to stop at zero speed reference. Maximum absolute values of the first and second derivatives of the speed reference trajectory are equal to 2200 rad/s² and 20000 rad/s³ correspondingly. Tracking of the speed reference trajectory requires rated motor torque.

3. From time $t=0.7$ s to $t=1.0$ s a constant load torque, equal to 100% of the motor rated value (7.0Nm), is applied.

Experimental set-up. The experimental tests have been carried out using a rapid prototyping station, which includes a Personal Computer acting as the Operator Interface during the experiments, a custom floating-point digital signal processor board based on TMS320C32 and a 50A/380VRMS three-phase inverter to feed the adopted IM. A symmetrical three-phase PWM technique with 10kHz switching frequency has been used to control the inverter. A vector controlled permanent magnet synchronous motor has been used to provide the load torque.

In the rapid prototyping station, two stator phase currents are measured by Hall-effect zero-field sensors. Only for monitoring purposes, the motor speed is measured by means of a 512 pulse/revolution incremental encoder. The sampling time for the controller has been set to 200 μ s. In order to get the discrete-time version of control algorithm the simple Euler method has been used.

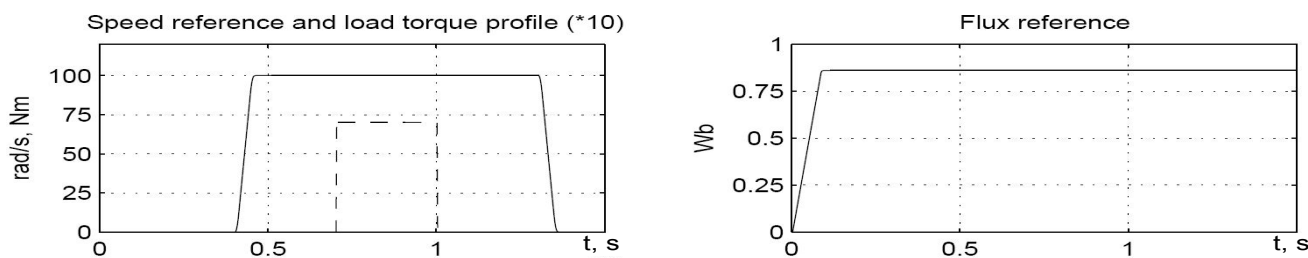


Fig. 1. Speed, flux references and load torque profile

Experimental and simulation results. A first set of experiments, whose results are reported in Figs. 2 a-c, has been performed in order to test the dynamic performance of the control algorithm during speed trajectory tracking and load torque rejection at high speed. The transient performance is characterized by a maximum speed tracking error of about 5 rad/s during speed reference variation and about 12 rad/s during load torque rejection transients. Steady-state speed tracking error is almost zero when constant reference speed and constant load torque are imposed. Estimated speed tracking error is close to the actual one even during transients, confirming that time-scale separation is achieved. Negligible current regulation errors are present during the experiments.

To validate the controller performance during experimental tests, comparison with simulation has been performed, under the same operating conditions of Fig. 1. In order to take into account the mechanical friction present in the experimental set-up, a linear friction torque $-v\omega/J$ is added in the simulated IM model and compensated with feed-forward actions in the controller. Friction coefficient value is $v = 0.0068\text{Nm}/(\text{rad/s})$.

Simulation results, reported in Figs. 3a-d, are similar to the experimental results in Fig. 2. The same maximum amplitude of both estimated and actual speed tracking error are obtained during load torque rejection. Note that in simulation tests, zero speed tracking error is achieved during steady-state conditions and during speed reference variation, while speed tracking error is not null in the experiments. This is mainly due to IM parameters uncertainties and inverter non-idealities such as dead-time effect and voltage commutations. Stator current and voltage profiles during experimental and simulation tests are comparatively shown in Figs. 2b-c and 3b-c. In Fig. 3d rotor flux errors are reported, showing that asymptotic flux amplitude regulation and field orientation are achieved.

Experimental transients during the same test as in Fig. 2, but with speed measurement (8) are shown in Fig. 4.

A second set of experiments has been performed to test the proposed solution when the persistency of excitation condition ((20) in [7]) fails or is near to fail. As it is well-known in the application-oriented literature [2] and according to the analysis in [7], the condition $\omega_0 = 0$ is critical and particularly significant in real-world applications.

In Fig. 5 a low-speed, regenerative condition (i.e. with negative output mechanical power) is considered. A speed reference profile with shape similar to Fig. 1, maximum speed of 10 rad/s and maximum time derivative of 220rad/s^2 has been imposed; -7.0Nm regenerative torque is applied. The nominal ω_0 is very close to zero with regenerative torque ($\omega_0 = 5.9\text{rad/s}$). No significant performance degradation is present in low-speed regenerative torque condition (Fig. 5) with respect to tests at high-speed (Fig. 2).

In Fig. 6 rejection of the rated load torque with zero speed reference is considered according to the operating sequence in Fig. 1. In this experiment nominal ω_0 goes from zero to 14.1rad/s and back. Again, the performances are very similar to previous cases; only after the load torque step down a small residual speed error can be noted, owing to lack of persistency of excitation.

Conclusions. A novel speed sensorless control for the full-order induction motor model with constant unknown load torque is designed on the basis of stator current measurements only. The proposed control algorithm is a “true” industrial sensorless solution since no simplifying assumptions (flux and load torque measurements) are required. The physically-based structure of the controller leads to a straightforward simplification if rotor speed is measured. Experiments and simulations of typical operating conditions demonstrate high dynamic performance during speed and flux tracking including load torque rejection, which is of the same order as for standard field-oriented solutions with speed measurement.

Acknowledgment. The authors should like to thank the CASY - Center for Research on Complex Automated Systems “G. Evangelisti”, University of Bologna, and EPA – Research and Development company, Kiev, for financial support and development of experimental installations for testing.

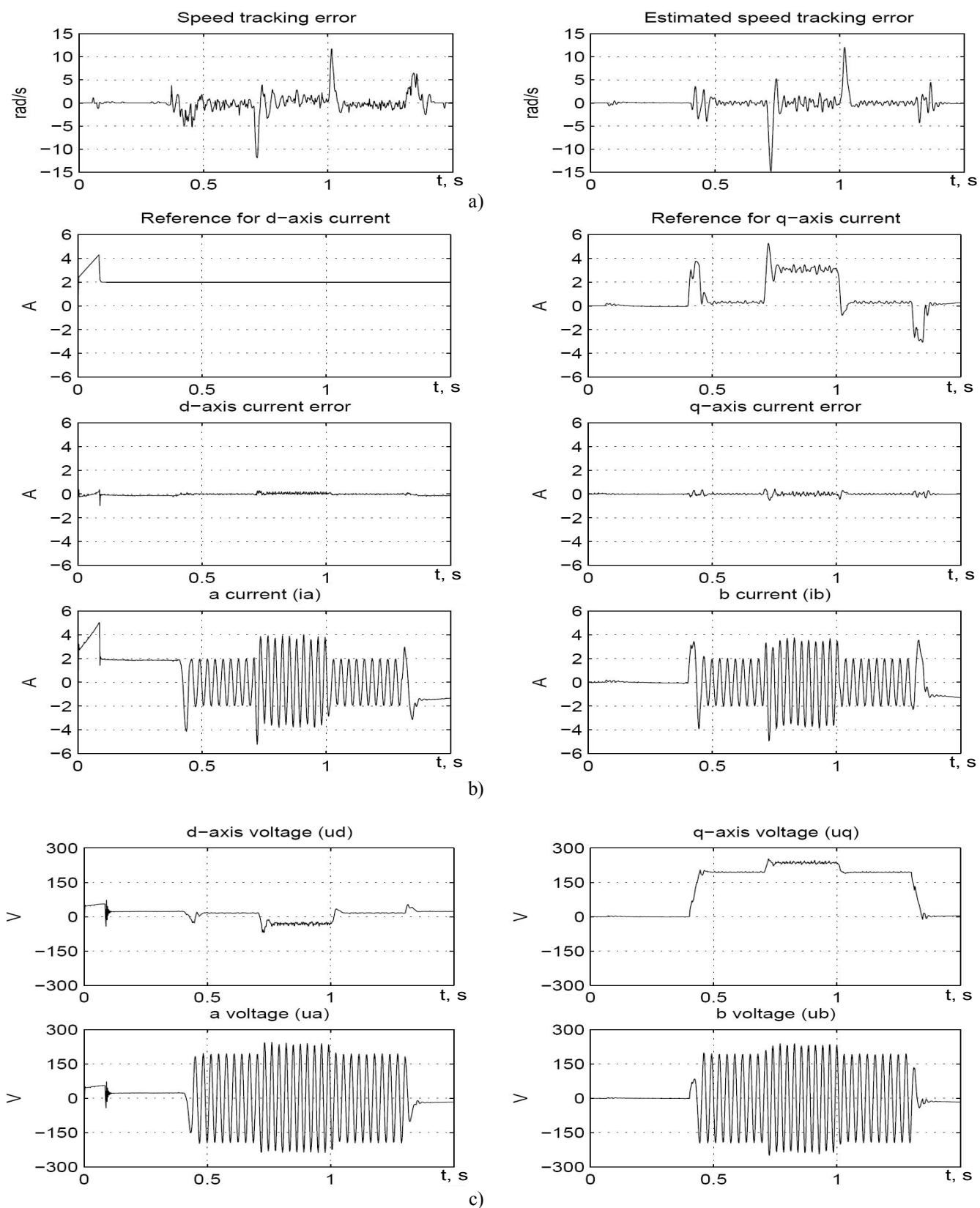


Fig. 2. Experimental results: dynamic behaviour of the sensorless controller with maximum speed reference equal to 100rad/s and applied load torque equal to 7.0Nm: a) speed errors; b) stator currents; c) stator voltages

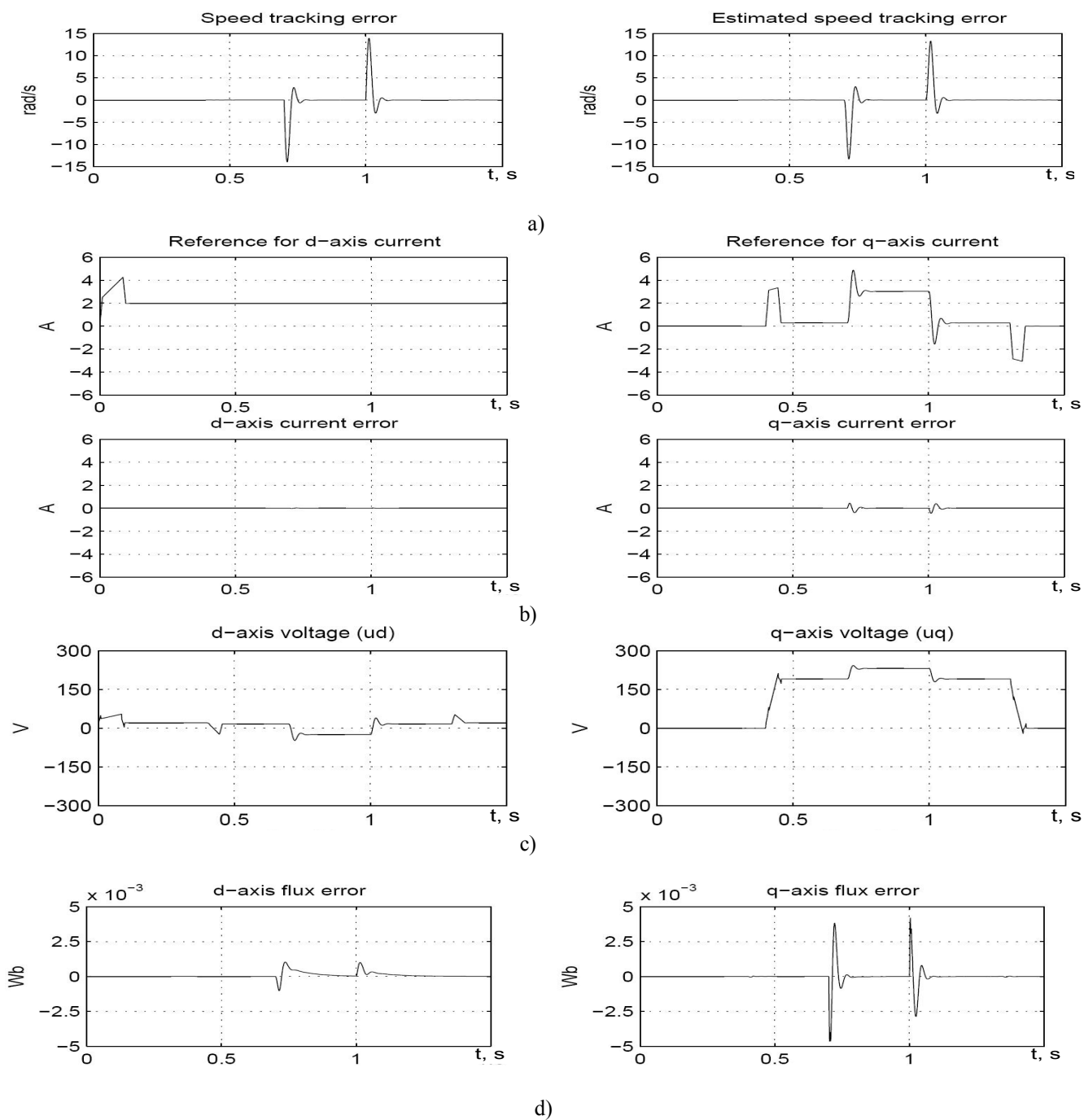


Fig. 3. Simulation results: dynamic behaviour of the sensorless controller: a) speed errors; b) stator currents; c) stator voltages; d) rotor flux errors

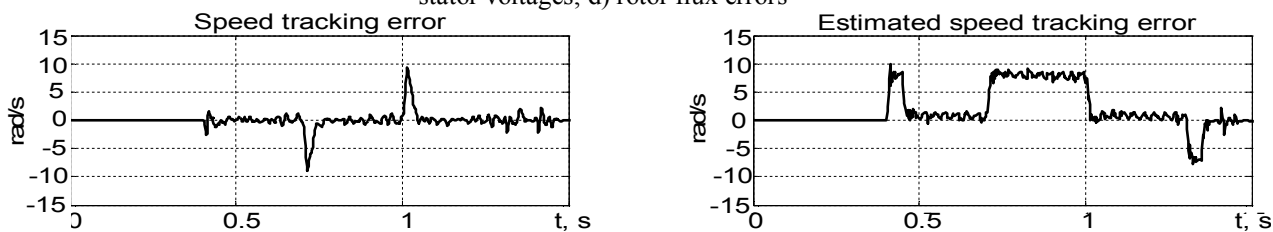


Fig. 4. Experimental results: dynamic behaviour of the sensed controller with maximum speed reference equal to 100rad/s and applied load torque equal to 7.0Nm

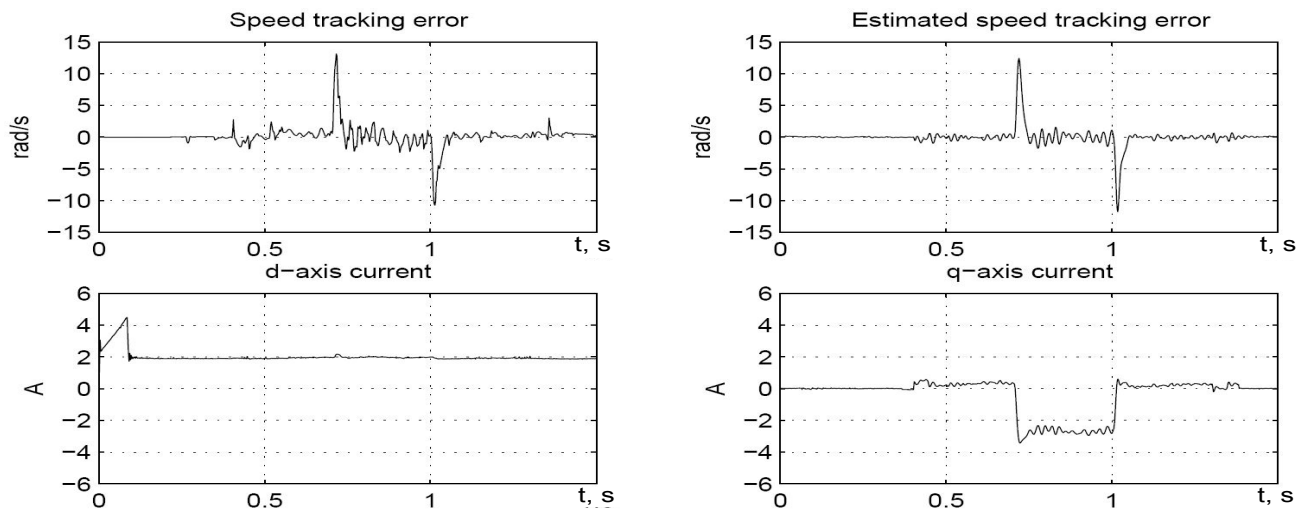


Fig. 5. Experimental results: dynamic behaviour of the sensorless controller with maximum speed reference equal to 10 rad/s and applied regenerative torque equal to -7.0Nm

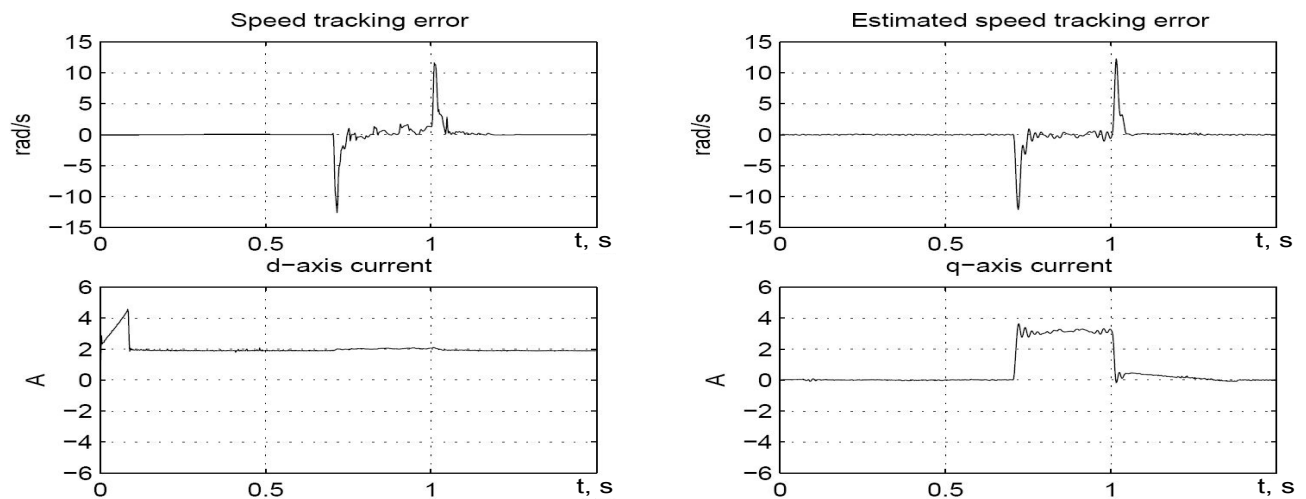


Fig. 6. Experimental results: dynamic behaviour of the sensorless controller with zero speed reference ($\omega^* = 0\text{ rad/s}$)

Reference.

1. Ilaş C., Bettini A., Ferraris L., Griva G. and Profumo F. Comparison of different schemes without shaft sensors for field oriented control drives // in Proc. of the 20th IEEE Conf. on Industrial Electronics. –1994. –P. 1579–1588.
2. Rajashekara K., Kawamura A. and Matsuse K. Sensorless control of AC motor drives. –IEEE Press, New York. –1996.
3. Vas P. Sensorless vector and direct torque control. –Oxford University Press. –1998.
4. Holtz J. Sensorless control of induction motor drives // in Proc. of the IEEE. –2002. –Vol. 90, No. 8. –P. 1359–1394.
5. Lorenz R. D. Practical issues and research opportunities when implementing zero speed sensorless control // in Proc. of the 5th International Conf. on Electrical Machines and Systems (ICEMS 2001). –Shenyang, China. –2001. –Vol. 1. –P. 1–10.
6. Kim Y., Sul S. and Park M. Speed sensorless vector control of induction motor using extended Kalman filter // IEEE Trans. on Industry Applications. –1994. –Vol. 30, No. 5. –P. 1225–1233.
7. Montanari M., Peresada S. and Tilli A. A speed-sensorless indirect field-oriented control for induction motors based on high gain speed estimation // Automatica. –2006. –Vol. 42. –P. 1637–1650.
8. Peresada, S. and Tonielli A. High-performance robust speed-flux tracking controller for induction motor // Int. Journal of Adaptive Control and Signal Processing. –2000. –Vol. 14. –P. 177–200.
9. Marino R., Peresada S. and Valigi P. Adaptive input – output linearizing control of induction motors // IEEE Trans. on Automatic Control. –1993. –Vol. 38, No. 2. –P. 208–221.